

Vortex Dynamics Near the Surface of a Bose-Einstein Condensate

U. Al Khawaja

Physics Department, United Arab Emirates University,
P.O. Box 17551, Al Ain, United Arab Emirates.
(Dated: May 23, 2019)

The center-of-mass dynamics of a vortex in the surface region of a Bose-Einstein condensate is investigated both analytically and numerically. Using a variational calculation, we obtain simple and accurate analytical results for the coordinates of the core of the vortex. We find that due to the inhomogeneity of the surface density, the vortex has a constant velocity component in the direction parallel to the surface of the condensate and an oscillatory component in the direction normal to the surface. This leads, in agreement with the experiments, to that the vortex precesses around the condensate. For large surface sizes, the dynamics of the vortex is similar to that of a freely falling object under the effect of the force of gravity. In the present case, the vortex falls toward the surface of the condensate, with a constant acceleration that is inversely proportional to the thickness of the surface region. We support our analytical results with a numerical simulation for the vortex motion obtained by solving numerically the time-dependent Gross-Pitaevskii equation. We get good agreement between the results of the variational calculation and those of the numerical calculation.

PACS numbers: 03.75.Fi, 67.40.-w, 32.80.Pj

I. INTRODUCTION

Following the experimental observation of vortices in Bose-Einstein condensates [1, 2, 3, 4, 5, 6, 7, 8, 9], vortex dynamics has been a subject of intensive interest [10, 11, 12, 13, 14, 15, 16, 17, 18, 19, 20, 21, 22]. Theoretical studies have been performed on the center-of-mass motion of the vortex core in the bulk of the condensate [10, 15, 22]. References [10, 22] have studied the dynamics of the core taking into account the dissipation from the thermal cloud. This leads to that the vortex spirals out of the condensate giving the vortex a finite lifetime in agreement with the experimental observations [2].

Once they reach the surface of the condensate, the vortices decay into surface excitations. It is also believed that vortices are created from instabilities of the surface excitations [19, 21, 23, 24, 25]. Hence, it is worth investigating the details of the dynamics of a vortex in the surface region of the condensate. We focus in the present paper on obtaining the trajectories of the vortex core in the surface region of a static condensate at zero temperature.

E. Lund et al. [26] have pointed out that near the surface of the condensate, the quadratic trapping potential can be approximated by a potential that is linear in distances normal to the surface. This leads to that the equilibrium density profile will be also linear in distances along the radius of the condensate except for distances very close to the Thomas-Fermi surface. An immediate question then arises: How will the vortex move in such an inhomogeneous density background? The fact that the density is linear makes it possible to perform an analytical treatment to the problem provided that the size of the core of the vortex is much less than the distance over which the background density varies significantly.

To answer the above question, we perform a variational calculation where we use an ansatz wavefunction that takes into account the equilibrium density profiles of both the background and the vortex. The variational parameters are the coordinates of the vortex core and their velocities in both directions; normal to the surface of the condensate and parallel to it. Equations of motion for these parameters are then derived from a lagrangian that corresponds to the time-dependent Gross-Pitaevskii equation.

Using a linear density profile for the background is an approximation that is not accurate very close to the Thomas-Fermi surface of the condensate. Thus our variational calculation is expected to be valid only away from the Thomas-Fermi surface. Furthermore, we neglect the internal dynamics of the core of the vortex. This is justified only away from the Thomas-Fermi surface where the size of the core is almost constant. Near the Thomas-Fermi surface, the core size grows significantly with the radial distance.

In the limit when the thickness of the surface region is much larger than the distance between the vortex core and the Thomas-Fermi surface, we obtain analytical solutions to the equations of motion. The solutions suggest that the vortex does indeed precess around the condensate. Coupled to this precessing motion, the vortex oscillates in the radial direction. Due to neglecting the dissipation from the thermal cloud, we obtain circular trajectories of constant radius.

In the following section we start by writing down an ansatz wavefunction. Using this wavefunction, we derive equations of motion for the variational parameters. Then we solve these equations to obtain the trajectories of the

vortex core. In Section III, we present the results of the numerical simulation of the vortex motion, and compare them with those of the variational calculation. In Section IV we summarize our main conclusions.

II. VARIATIONAL APPROACH

In this section we calculate the lagrangian of a vortex moving near the surface of a static Böse-Einstein condensate. Taking the coordinates of the core of the vortex and its center-of-mass velocity as time-dependent variational parameters, we calculate equations of motion for these parameters. Interesting solutions are then obtained and discussed.

The dynamics of the Böse-Einstein condensate is described by the Gross-Pitaevskii equation

$$\frac{\hbar^2}{2m} \mathbf{r}^2 + V(\mathbf{r}) + g j(\mathbf{r}; t) \hat{j} \quad (r; t) = i\hbar \frac{\partial}{\partial t} (r; t) : \quad (1)$$

Here g is the effective two-particle interaction which is proportional to the s-wave scattering length a according to $g = 4\pi a \hbar^2/m$, where m is the mass of an atom, and j is the equilibrium chemical potential. The harmonic trapping potential $V(\mathbf{r})$ is given by

$$V(\mathbf{r}) = \frac{1}{2} m \omega_0^2 \mathbf{r}^2 ; \quad (2)$$

where ω_0 is the characteristic frequency of the trap. Here, we take for simplicity $V(\mathbf{r})$ to be isotropic, although this is not necessary in the limit which we take next.

For distances near the surface of the condensate, the quadratic trapping potential $V(\mathbf{r})$ can be approximated by a linear potential [26]

$$V(\mathbf{r}) \approx V(R) + F \mathbf{x} ; \quad (3)$$

where \mathbf{x} is a coordinate normal to the surface of the condensate, R is the Thomas-Fermi radius given by $V(R) = 0$, and $F = m \omega_0^2 R$ is a force constant. This suggests a planar geometry in which the surface of the condensate is approximated by an infinite plane. The x -coordinate will be normal to the plane while the y and z coordinates will be parallel to it. The origin of this coordinate system is then shifted from the center of the condensate to the surface. In this planar geometry, the Gross-Pitaevskii equation takes the form

$$\frac{\hbar^2}{2m} \mathbf{r}^2 + F \mathbf{x} + g j(\mathbf{r}; t) \hat{j} \quad (r; t) = i\hbar \frac{\partial}{\partial t} (r; t) : \quad (4)$$

It should be noted here that the coordinates \mathbf{r} and \mathbf{x} are measured from the shifted origin which is at the surface. The bulk of the condensate occupies the region $x < 0$. The equilibrium density profile $n_0(x) = |j(x)|^2$ is obtained from the last equation by setting the time derivative to zero

$$\frac{\hbar^2}{2m} \frac{d^2}{dx^2} + F \mathbf{x} + g n_0(x) \frac{d}{dx} \frac{p}{n_0(x)} = 0 : \quad (5)$$

For large negative values of x , the kinetic energy operator can be neglected leading to the Thomas-Fermi equilibrium density $n_0(x) = (F/g)x$ [26, 27]. The kinetic energy operator is important only near $x = 0$.

We consider a vortex with a core located at $\mathbf{r} = \mathbf{x}_0(t)\hat{x} + \mathbf{y}_0(t)\hat{y}$ and axis along the z -direction. The vortex has a center-of-mass velocity $\hat{v} = v_x(t)\hat{x} + v_y(t)\hat{y}$. For the sake of obtaining analytical results, we perform the present variational calculation in the linear region of the equilibrium condensate density profile, i.e. for $x < 0$. The effect of the nonlinear region near $x = 0$ is accounted for in the next section where we solve numerically the time-dependent Gross-Pitaevskii equation, Eq. (1).

Our trial wavefunction is given by

$$(r; t) = \frac{s}{\sqrt{\frac{F x}{g}}} () \exp(i\phi) \exp[i(m\hbar)(xv_x + yv_y)] : \quad (6)$$

Here, the first factor on the right hand side corresponds to the linear background density. The second and third factors correspond to the density and phase of a vortex in a uniform background, respectively. The polar coordinates

$= \frac{p}{(x - x_0(t))^2 + (y - y_0(t))^2}$ and have the core of the vortex as their origin. The last factor represents the center-of-mass velocity of the vortex. The vortex density profile is taken as [28]

$$^2(\rho) = \frac{1}{2^2 + \rho^2}; \quad (7)$$

where $\rho = \frac{p}{8\pi n_0(x_0)}$ is the coherence length of the condensate calculated at x_0 . A good deal of the vortex dynamics can be obtained without specifying the details of ρ . It turns out, for instance, that the y -component of the vortex motion is independent of the functional form of ρ .

Due to the nonlocal nature of the vortex excitation, the energy of the vortex diverges logarithmically with the size of the system. To be able to perform our variational calculation for a finite and constant number of atoms N , we consider a cylinder of radius b and length l such that the cylinder axis coincides with the vortex axis. The fact that we restrict the number of atoms within the cylinder to be constant, is guaranteed by requiring $\langle r; t \rangle$ to be normalized to N . This leads to

$$\langle r; t \rangle = \frac{r}{\frac{N}{N_1}} \frac{r}{\frac{x}{x_0(t)}} (\rho) \exp(i\theta) \exp[i(m\hbar)(xv_x + yv_y)]; \quad (8)$$

where

$$N_1 = \frac{Z_b}{d} \frac{Z_2}{d} : \quad (9)$$

The lagrangian that corresponds to Eq. (4) reads

$$L[\rho; \dot{r}] = \frac{Z}{dr} \frac{ih}{2} \dot{r} (\rho) \frac{\partial}{\partial t} \dot{r} (\rho) \frac{\partial}{\partial t} \dot{r} (\rho) E[\rho; \dot{r}]; \quad (10)$$

where $E[\rho; \dot{r}]$ is the energy functional given by

$$E[\rho; \dot{r}] = \frac{Z}{dr} \frac{h^2}{2m} \dot{r} (\rho) \dot{r} (\rho) + F x \dot{r} (\rho) \dot{r} (\rho) + \frac{1}{2} g \dot{r} (\rho) \dot{r} (\rho) : \quad (11)$$

Using the trial wavefunction Eq. (8), we calculate the lagrangian per atom to get

$$\begin{aligned} L/N = & \frac{h^2}{8m} + \frac{gN N_2}{2N_1^2} \frac{1}{x_0^2} \\ & \frac{m N_3}{N_1} v_x + \frac{h N_4}{N_1} y_0 \quad \frac{h N_4}{N_1} v_y + \frac{F N_3}{N_1} \frac{1}{x_0(t)} \\ & \frac{m}{2} (v_x^2 + v_y^2) \quad m y_0 \quad \frac{h^2 N_5}{2m N_1} \quad \frac{gN N_6}{2N_1^2} \\ & F x_0 \quad m v_x x_0; \end{aligned} \quad (12)$$

where $R_b = d^2$, $R_2 = d^2 \sin^2$, $R_3 = d^2 \sin^2$, $R_4 = d^2 \sin^2$, $R_5 = d^2 + 2^2 \cos^2 = 2 + 2^2 \cos^2$, $R_6 = d^4$:

The dot on y_0 , v_x , and v_y denotes derivative with respect to time and $\dot{\rho} = \partial \rho / \partial t$. The equations of motion of the variational parameters are derived from the Euler equations of the lagrangian. For convenience, we present these equations in terms of scaled quantities. We scale length to $\tilde{r} = (h^2/mF)^{1/3}$, time to $\tilde{t} = m^2/h$, energy to $\tilde{E} = h^2/m^2$, and density to $(2\pi)^2 N/N_1$. In these units, the lagrangian per atom takes the following dimensionless form

$$\tilde{L}/N = \frac{1}{8} + \frac{N_2}{N_1} \frac{1}{\tilde{x}_0^2(t)} \quad !$$

$$\begin{aligned}
& \frac{\tilde{N}_3}{\tilde{N}_1} (1 + \tilde{v}_x(t)) - \frac{1}{2} \tilde{v}_y(t) + \frac{1}{2} \tilde{y}_0(t) - \frac{1}{\tilde{x}_0(t)} \\
& \frac{\tilde{N}_5}{2\tilde{N}_1} + \frac{\tilde{N}_6}{\tilde{N}_1} + \frac{1}{2} (\tilde{v}_x^2(t) + \tilde{v}_y^2(t) + 2\tilde{y}_0(t)\tilde{v}_y(t)) \\
& 1 + \tilde{v}_x(t) \tilde{x}_0(t); \tag{13}
\end{aligned}$$

where the tilde denotes scaled quantities as described above. It is important to note here that the scattering length disappears completely in these units. This is only possible in our infinite plane geometry approximation. The equations of motion, thus, read

$$\frac{\tilde{N}_3}{\tilde{N}_1 \tilde{x}_0^2(t)} - 1 \tilde{x}_0(t) + \tilde{v}_x(t) = 0; \tag{14}$$

$$\begin{aligned}
& \frac{1}{4} + 2 \frac{\tilde{N}_2}{\tilde{N}_1} - \frac{1}{\tilde{x}_0^3(t)} - 1 + \tilde{v}_x(t) \\
& + \frac{\tilde{N}_3}{\tilde{N}_1} (1 + \tilde{v}_x(t)) - \frac{1}{2} \tilde{v}_y(t) + \frac{1}{2} \tilde{y}_0(t) - \frac{1}{\tilde{x}_0^2(t)} = 0; \tag{15}
\end{aligned}$$

$$\tilde{y}_0(t) + \frac{1}{2\tilde{x}_0(t)} \tilde{v}_y(t) = 0; \tag{16}$$

$$2\tilde{v}_y(t) + \frac{\tilde{x}_0(t)}{\tilde{x}_0^2(t)} = 0; \tag{17}$$

From the last two equations, we obtain the following simple result

$$\tilde{y}_0(t) = 0; \tag{18}$$

This is a general result in the sense that it neither depends on the functional form of \tilde{v}_x nor it depends on the size of the system through the upper limit of the radial integration \tilde{b} . We solve numerically Eqs. (14)–(17) for given values of \tilde{b} . The results are shown in Fig. 1. While the vortex motion is uniform in the y -direction, it is oscillatory in the x -direction with a frequency that decreases with increasing system size \tilde{b} .

This oscillatory solution can be derived analytically from the equations of motion in the limit $\tilde{b} \rightarrow \tilde{x}_0$. For our infinite system, this is the relevant limit to take. To obtain the equations of motion in this limit, we expand the integrals $\tilde{N}_1 \dots \tilde{N}_6$ in powers of \tilde{b} to get: $\tilde{N}_1' \sim \tilde{b}^2$, $\tilde{N}_2' \sim \tilde{b}^4 = 4 - 2\tilde{b}^{-2}$, $\tilde{N}_3' \sim \tilde{b}^4 = 4 - \tilde{b}^{-2}$, $\tilde{N}_4' \sim \tilde{b}^2 = 2$, $\tilde{N}_5' \sim 3 = 4 + \log(\tilde{b}^2 = 2^{-2})$, and $\tilde{N}_6' \sim \tilde{b}^2 + 2^{-2}$. In this limit, Eqs. (14) and (15) reduce to

$$\frac{\tilde{N}_3}{\tilde{N}_1} \frac{d}{dt} \frac{1}{\tilde{x}_0(t)} + \tilde{v}_x(t) = 0; \tag{19}$$

$$2\tilde{N}_2 + \tilde{N}_3 \tilde{x}_0(t) - 1 + \tilde{v}_x = 0; \tag{20}$$

Equations (19) and (20) lead to the following second order differential equation for $\tilde{x}_0(t)$

$$\frac{d^2}{dt^2} \frac{1}{\tilde{x}_0(t)} + \frac{8}{\tilde{b}^2} \frac{1}{\tilde{x}_0(t)} + \frac{4}{\tilde{b}^2} = 0; \tag{21}$$

For the initial conditions $\tilde{x}_0(0) = \tilde{X}_0$ and $\dot{\tilde{x}}_0(0) = 0$, the solution of this equation is

$$\tilde{x}_0(t) = \frac{1}{1 + 2 + \tilde{X}_0^{-1} + 1 = 2 \cos \frac{p\sqrt{8}}{\tilde{b}} t}; \tag{22}$$

It turns out that this simple solution is an accurate solution of the equations of motion, Eqs. (14)–(17), as is shown in Fig. 2. As we will also see in the next section, this solution agrees well with the numerical calculations.

Equations (18) and (22) show that the vortex will be falling to the surface of the condensate and then bouncing back from it. This analogy with objects falling under the influence of gravity can be seen more clearly by expanding the solution Eq. (22) for large \tilde{b} (or small t)

$$\mathbf{x}_0(t) \approx \mathbf{x}_0 + \frac{1}{2} \mathbf{a}_v t^2; \quad (23)$$

where $\mathbf{a}_v = 2\mathbf{x}_0 \tilde{b}^{-2}$ is a constant acceleration. This is analogous to the equation of the vertical coordinate of a freely falling object. In the present case, the vortex falls to the surface with the acceleration \mathbf{a}_v . For an infinite system, we have $\tilde{b} \gg 1$, $\mathbf{a}_v = 0$, and $\mathbf{x}_0 = \mathbf{x}_0$. Since the result Eq. (18) is general and thus is true in this limit, we conclude the general result that the trajectory of the vortex will be a straight path parallel to the surface of the condensate. In a spherical condensate, this leads to conclude that the vortex will move in a circular path along the circumference of the condensate where the plane of the circle is perpendicular to the axis of the vortex.

Depending on the initial location of the vortex core from the Thomas-Fermi surface, there are two possibilities for the vortex motion. If the thickness of the surface layer is much larger than the initial position of the core of the vortex, $\tilde{b} \ll \mathbf{x}_0$, then the vortex will just precess around the condensate. It will not come close to the Thomas-Fermi surface to decay there. Alternatively, if the thickness is of the order of the initial position, $\tilde{b} \approx \mathbf{x}_0$, the vortex will fall to the surface and decay there by generating surface excitations. In the first case, the frequency of precession around the condensate is $\mathbf{v}_y = \tilde{R} = 1/2\tilde{R}\mathbf{x}_0$, where we have used the equilibrium value for \mathbf{v}_y from Eq. (27) below. In the second case, the time needed for the vortex to reach the surface, according to Eq. (23), equals \tilde{R}/\mathbf{a}_v . For a typical condensate $\tilde{R} = 10a_0 = 10^6$ m and $\mathbf{x}_0 = 10^8$ s⁻¹, where $a_0 = \hbar/m$ is the characteristic length of the harmonic trapping potential. This leads to that $\tilde{R} = (\hbar^2/mF)^{1/3} = (a_0/\tilde{R})^{1/3}a_0 = 0.46a_0$ and $\tilde{R} = (\hbar^2/a_0^2) = \mathbf{x}_0 = 0.2 = 10^8$ s⁻¹. Taking $\tilde{b} = \tilde{R}$, and $\mathbf{x}_0 \approx 1$, we get $\mathbf{a}_v = 10^4$ m/s², frequency of precessing around the condensate $\approx 5 \times 10^8$ s⁻¹, and time to reach the condensate ≈ 0.2 s.

It is also interesting to obtain the equilibrium values of the variational parameters. These can be obtained by minimizing the energy functional with respect to the variational parameters. In order to obtain the energy change due to the presence of the vortex, we have to subtract from the vortex energy the energy of the background [29]

$$E_{vf} = \frac{Z_b}{d} + \frac{Z_2}{d} - \frac{1}{2} g \frac{N_x^2}{N_1 x_0} + F \frac{N_x}{N_1 x_0} \mathbf{x} : \quad (24)$$

The terms on the right hand side of this equation represent the mean-field and trapping potential energies of the vortex-free background within a cylinder of radius b and length l . The energy functional can thus be readily obtained from Eq. (13) by setting time derivatives to zero, multiplying by -1 , and then subtracting the energy of the background

$$\begin{aligned} E_v - N &= \frac{1}{8} + \frac{4N_2}{4N_1} \frac{\tilde{b}^4}{x_0^2(t)} - \frac{1}{x_0^2(t)} \\ &+ \frac{4N_3}{4N_1} \frac{\tilde{b}^4}{N_1} \frac{N_4 v_y(t)}{N_1} - \frac{1}{x_0(t)} \\ &+ \frac{N_5}{2N_1} + \frac{N_6}{N_1} \frac{\tilde{b}^2}{N_1} + \frac{1}{2} (v_x^2(t) + v_y^2(t)) \\ &+ \frac{N_1}{N_1} \frac{\tilde{b}^2}{N_1} x_0(t) : \end{aligned} \quad (25)$$

In the large \tilde{b} limit, this reduces to

$$E_v - N = \frac{1}{8} Z^2 \frac{1}{x_0^2(t)} - \frac{1}{2} v_y(t) \frac{1}{x_0(t)} + \frac{1}{2} v_x^2(t) + v_y^2(t) : \quad (26)$$

It turns out that the energy functional is independent of $v_0(t)$ as expected due to the symmetry of the system in the y -direction. Setting to zero the first derivatives of E_v with respect to v_y and x_0 and then solving the resulting

equations for v_y and x_0 gives

$$v_y(t) = \frac{h}{2m x_0(t)}; \quad (27)$$

and

$$x_0(t) = 4 : \quad (28)$$

Equation (27) suggests that, at equilibrium, the vortex will be rolling on the surface of the condensate with a rolling speed that is half of superuid speed at a distance $|x_0|$ from the core.

III. NUMERICAL SOLUTION

In the previous section we have obtained several features of the dynamics of the vortex analytically using a variational calculation. In the present section, we solve the time-dependent Gross-Pitaevskii equation, Eq. (1), numerically. We find agreement with the above analytical results and obtain new features for distances near the Thomas-Fermi surface where the variational calculation is not expected to be accurate. Writing Eq. (1) in the same units used in the previous section, it takes the following dimensionless form

$$\frac{1}{2} r^2 + \mathbf{x} + j^2(\mathbf{r}; t) \hat{\psi}(\mathbf{r}; t) = i \frac{\partial}{\partial t} \hat{\psi}(\mathbf{r}; t); \quad (29)$$

where r^2 is scaled to $4/a^2$.

We start by solving the time-independent Gross-Pitaevskii equation

$$\frac{1}{2} \frac{\partial^2}{\partial \mathbf{x}^2} + \mathbf{x} + j_0^2(\mathbf{x}) \hat{\psi}_0(\mathbf{x}) = 0 : \quad (30)$$

We use the imaginary-time evolution method to solve this equation. The resulting density $n_0(\mathbf{x})$ is the background density profile for the vortex. Then we multiply this density by a density profile of a vortex in a uniform background, namely j^2 given by Eq. (7). The next step could be an immediate use of the resulting density profile as an initial condition for solving the time-dependent Gross-Pitaevskii equation. However, we should notice that j of Eq. (7) is only a trial function and is not the exact density profile of the vortex. When we simulated the dynamics of the vortex using this density profile, the size of the core of the vortex acquired a breathing oscillation during the vortex motion. This oscillation produced circular density waves emitted from the vortex core through the background. Since we are interested mainly in the center-of-mass motion of the vortex, it is necessary to use the exact density profile of the vortex. This can be obtained by evolving in imaginary time the density n_0 . In other words, we resolve Eq. (30) with $\hat{\psi}_0$ as an initial wavefunction. The resulting profile contains now the exact background and vortex core structure as is shown in Fig. 3. This profile is then used as the initial profile for the time-dependent Gross-Pitaevskii equation. We found that density waves emerging from the vortex core have now disappeared.

In Fig. 4 we show the density profile of the vortex and background at different times. To compare with the previous analytical results, we plot in Figs. 5-6 the coordinates of the core $x_0(t)$ and $y_0(t)$ as a function of time, and in Fig. 7 we plot the trajectory $x_0(t)$ versus $y_0(t)$. On the same plots, we show the predicted trajectories of the analytical calculation. Excellent agreement is obtained for the y -component of the motion for large x_0 . For the x -component of the motion, we needed to fit the analytical prediction Eq. (22) with the numerical result. The fitting parameter is δ . In solving the time-dependent Gross-Pitaevskii equation, δ enters in the numerical solution through the boundary conditions. In the ideal situation, we should have large enough background to get dynamics that is independent of δ . Since in the present situation the numerical calculation is done on a finite grid, a finite value of δ is then needed to match the analytical results with the numerical ones.

In the numerical simulation shown in Fig. 4 we notice that the vortex, instead of bouncing back from the surface of the condensate as predicted by the variational calculation, it decays at the surface. This is due to the density fluctuations. When the vortex is close to the surface, these density fluctuations become of the same magnitude of the density profile of the vortex and thus destroy it.

In the previous section, we concluded that, in an infinite system, the vortex will move in a path that is parallel to the surface of the condensate. To verify this conclusion, we plot in Fig. 8 the x -component of the vortex trajectory for increasing values of δ . We see clearly that by increasing δ the oscillatory motion of the vortex will have a smaller amplitude and frequency as expected. For a large enough δ , the oscillation disappears and the vortex moves in a straight line parallel to the surface.

We have also calculated the size of the core of the vortex along both the x and y -directions. This is plotted in Fig. 9. This figure shows that the core sizes change slightly for large x_0 and grows rapidly near $x = 0$. The fact that the core sizes grow by approaching the Thomas-Fermi surface can be understood by noting that the core size is of the order of $\sqrt{\rho}$ which is inversely proportional to the condensate density. In the previous section, we performed the calculation in the large x_0 limit and neglected the dynamics of the size of the core. It is clear now that ignoring the core dynamics is indeed justified for large x_0 .

IV. CONCLUSIONS

We have calculated the trajectories of a vortex near the surface of a Bose-Einstein condensate. We performed this both analytically using a variational calculation and numerically using a numerical simulation of the time-dependent Gross-Pitaevskii equation.

The variational calculation was performed using the linear Thomas-Fermi density profile of the vortex background. This is accurate for distances away from the Thomas-Fermi surface of the condensate as is shown in Fig. 3. We obtained simple and accurate analytical results that suggest similarity between vortex dynamics and freely falling objects under the influence of gravity. Specifically, we found that the component of the vortex core velocity that is parallel to the surface of the condensate, is constant. We found also that the vortex will be accelerating toward the surface of the condensate with a constant acceleration that depends inversely on the size of the system. For an infinite system, this acceleration vanishes indicating that the vortex will move only parallel to the surface of the condensate. We found also that for realistic situations where the size of the surface region is finite, the vortex will be oscillating in the direction normal to the surface. This means that in addition to precessing around the condensate, the vortex will have a radial oscillatory motion.

Furthermore, we have calculated the equilibrium positions and velocities of the vortex. We found that in the direction parallel to the surface, the equilibrium speed of the core is half the superfluid velocity at the surface. This is similar to rolling rigid objects on surfaces, but in the latter case the center of mass speed (vortex core speed in our case) equals the tangential speed at the surface of the object and not half of it as in our case. The factor of half arises in the present case from the inhomogeneity of the density of the background.

To support our analytical results, we have simulated the motion of the vortex by solving numerically the time-dependent Gross-Pitaevskii equation. We have obtained very good agreement between the results of the variational calculation and the numerical results for large distances from the surface. For distances very close to the surface, the analytical results deviate from the numerical ones due to the fact that, in the variational calculation, we have used the Thomas-Fermi approximation which breaks down at the surface. We verified numerically that by increasing the size of the system, the vortex takes longer time to reach the surface, which can be interpreted as it has lower acceleration toward the surface, as is predicted by the analytical results. We have also calculated numerically the size of the core of the vortex in both directions, normal and parallel to the surface. It turned out that for large distances from the surface, the core size is almost constant. This supports neglecting the core dynamics in the variational calculation.

[1] M.R. Matthews et al., *Phys. Rev. Lett.* **83**, 2498 (1999).
 [2] B.P. Anderson et al., *Phys. Rev. Lett.* **85**, 2857 (2000).
 [3] K.W. Madison, F. Chevy, W.W. Ohlmann, and J. Dalibard, *Phys. Rev. Lett.* **84**, 806 (2000).
 [4] K.W. Madison, F. Chevy, and J. Dalibard, *Phys. Rev. Lett.* **86**, 4443 (2001).
 [5] P.C. Haljan, I. Coddington, P. Engels, and E.A. Cornell, *Phys. Rev. Lett.* **87**, 210403 (2001).
 [6] C.Raman et al., *Phys. Rev. Lett.* **87**, 210402 (2001).
 [7] J.R. Abo-Shaeer, C.Raman, J.M. Vogels, and W. Ketterle, *Science* **292**, 476 (2001).
 [8] J.R. Abo-Shaeer, C.Raman, and W. Ketterle, *Phys. Rev. Lett.* **88**, 070409 (2002).
 [9] E.H. Odby et al., *Phys. Rev. Lett.* **88**, 010405 (2001).
 [10] P.O. Fedichev and G.V. Shlyapnikov, *Phys. Rev. A* **60**, R1779 (1999).
 [11] D. Butts and R. Okhsar, *Nature* (London) **397**, 327 (1999).
 [12] Y. Castin and R. Dum, *Eur. Phys. J. D* **7**, 399 (1999).
 [13] F. Dalfovo, S. Giorgini, L.P. Pitaevskii, and S. Stringari, *Rev. Mod. Phys.* **71**, 463 (1999).
 [14] D.L. Feder, C.W. Clark, and B.I. Schneider, *Phys. Rev. Lett.* **82**, 4956 (1999).
 [15] A.L. Fetter, *Phys. Rev.* **140**, A429 (1965).
 [16] A.L. Fetter and A.A. Svidzinsky, *J. Phys.: Condens. Matter* **13**, R135 (2001).
 [17] K.W. Madison, F. Chevy, W.W. Ohlmann, and J. Dalibard, *J. Mod. Opt.* **47**, 2715 (2000).
 [18] A.A. Svidzinsky and A.L. Fetter, *Phys. Rev. Lett.* **84**, 5919 (2000).
 [19] J. Anglin, *Phys. Rev. Lett.* **87**, 240401 (2001).

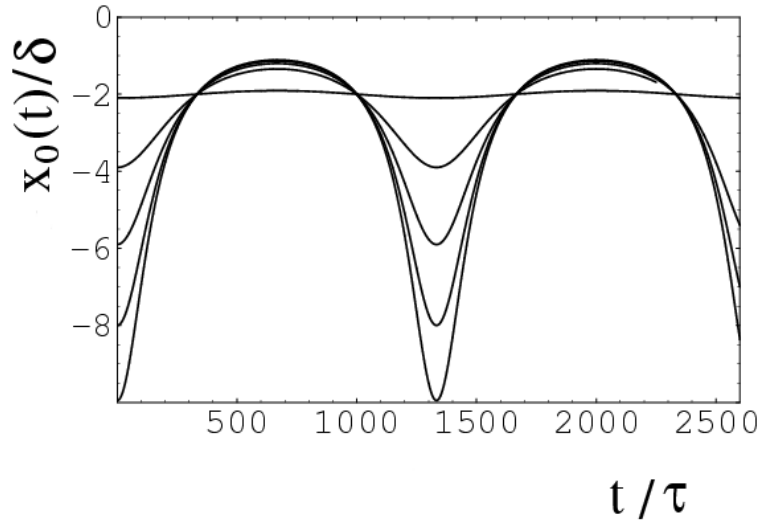


FIG. 1: The solution of the equations of motion Eqs. (14)–(17) for different initial values of x_0 and y_0 . The curves correspond to $(x_0(0), y_0(0)) = (-10, -10), (-8, -8), (-6, -6), (-4, -4), (-2, -2)$. We have used for all these curves $\delta = 600$.

- [20] J. Anglin, Phys. Rev. A 65, 063611 (2002).
- [21] U. Al Khawaja, Phys. Rev. A 68, 063614 (2003).
- [22] R. A. Duine, B. W. A. Leurs, and H. T. C. Stoof, cond-mat/0311651
- [23] F. Dalfovo and S. Stringari, Phys. Rev. A 63, 011601 (2001).
- [24] T. Isoshima and K. Machida, Phys. Rev. A 60, 3313 (1999).
- [25] A. E. Muryshev and P. O. Fedichev, cond-mat/0106462.
- [26] E. Lundh, C. J. Pethick, and H. Smith, Phys. Rev. A 55, 2126 (1997).
- [27] G. Baym and C. J. Pethick, Phys. Rev. Lett. 76, 6 (1996).
- [28] A. L. Fetter, in *Lectures in Theoretical Physics*, eds. K. T. M. Mahanthappa and W. E. Brittin (Gordon and Breach, N.Y., 1969), Vol. XIB, p. 351.
- [29] C. J. Pethick and H. Smith, *Bose-Einstein Condensation in Dilute Gases*, (Cambridge 2002).
- [30] D. L. Feder, C. W. Clark, and B. I. Schneider, Phys. Rev. A 61, 011601 (2000).
- [31] M. Tsubota, K. Kasamatsu, and M. Ueda, Phys. Rev. A 65, 023603 (2002).
- [32] A. A. Penckwitt, R. J. Ballagh, and C. W. Gardiner, Phys. Rev. Lett. 89, 260402 (2002).
- [33] U. Al Khawaja, C. J. Pethick, and H. Smith, Phys. Rev. A 60, 1507 (1999).
- [34] A. A. Svidzinsky and A. L. Fetter, Phys. Rev. A 62, 063617 (2000), 5919 (2000).

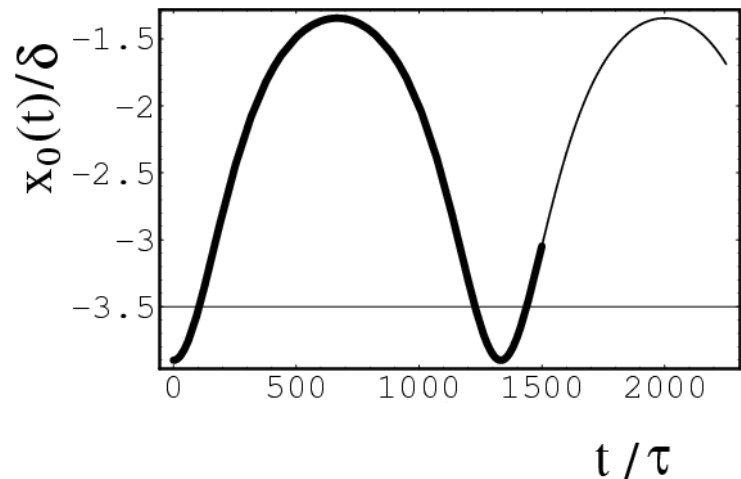


FIG. 2: The light curve is the numerical solution of the equations of motion Eqs. (14)–(17). The thick curve is an analytical solution of the equations of motion in the limit $\delta \rightarrow 1$, which is given by Eq. (22). The two curves lie on the top of each other.

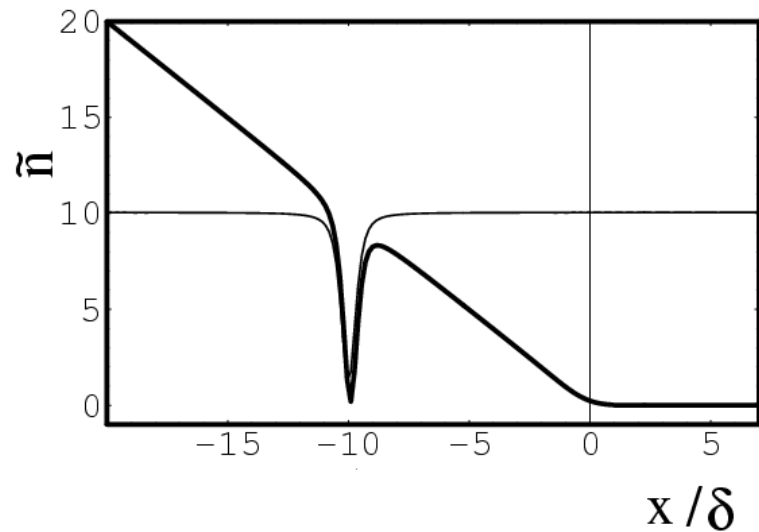


FIG. 3: Density profile $n = j^2$ of the x and y-cross sections of a vortex with core located at $(x_0; y_0) = (-10; 10)$. The thick curve corresponds to the x-cross section and the light curve corresponds to the y-cross section. The density is in units of $1=4 \text{ a}^2$.

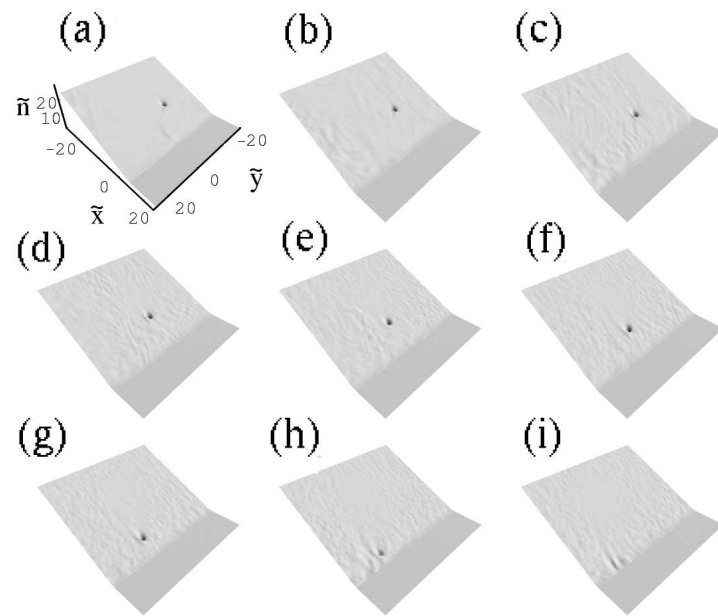


FIG. 4: Density profile of the vortex and the background. Time increases starting from (a). The initial vortex core coordinates are $(\tilde{x}_0, \tilde{y}_0) = (-10, -10)$.

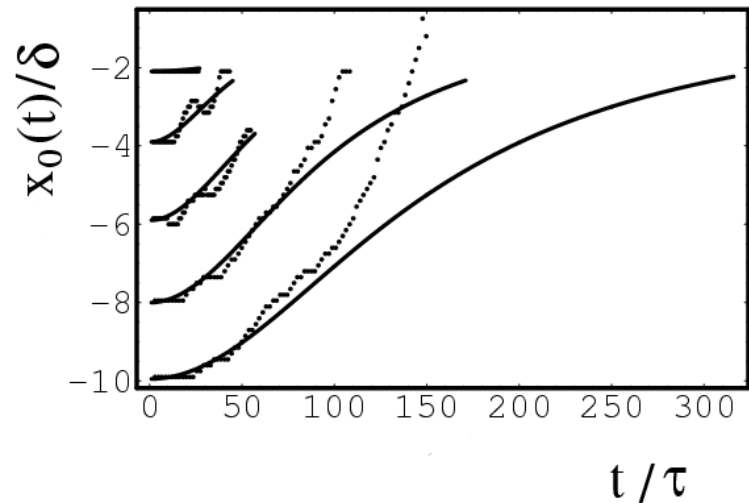


FIG. 5: The x -coordinate of the vortex core, $x_0(t)$, as a function of time. The dots are the results of the numerical simulation of the time-dependent Gross-Pitaevskii equation, Eq. (1). The solid curves are the results of the variational calculation obtained by solving the equations of motion Eqs. (14)–(17). The values of δ used to calculate the analytical curves, equal starting from the lowest curve: 620, 350, 200, 100, 50.

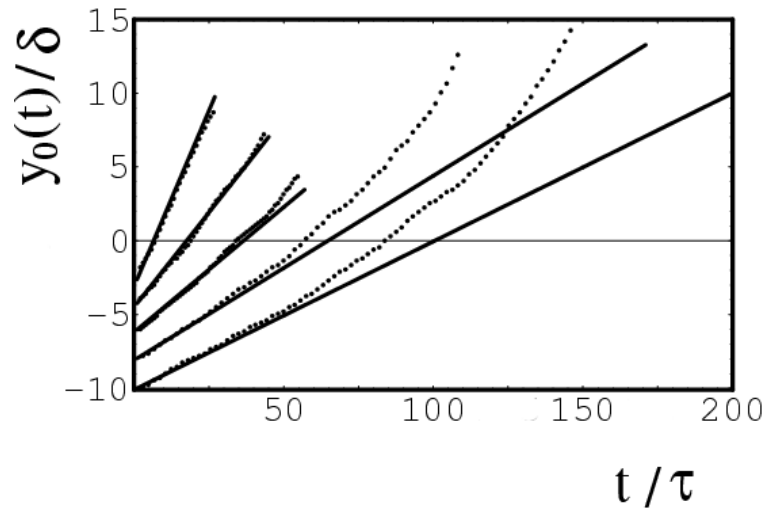


FIG . 6: The y-coordinate of the vortex core, $y_0(t)$, as a function of time. The dots are the results of the numerical simulation of the time-dependent Gross-Pitaevskii equation, Eq. (1). The solid curves are the results of the variational calculation obtained by solving the equations of motion Eqs. (14)–(17). The values of δ used to calculate the analytical curves, equal starting from the lowermost curve: 620, 350, 200, 100, 50.

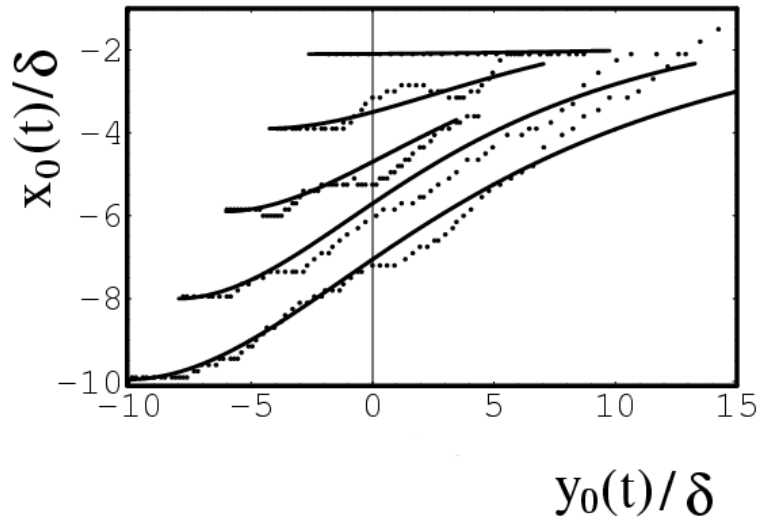


FIG . 7: The trajectory of the vortex core; $x_0(t)$ as a function of $y_0(t)$. The dots are the results of the numerical simulation of the time-dependent Gross-Pitaevskii equation, Eq. (1). The solid curves are the results of the variational calculation obtained by solving the equations of motion Eqs. (14)–(17). The values of δ used to calculate the analytical curves, equal starting from the lowest curve: 620, 350, 200, 100, 50.

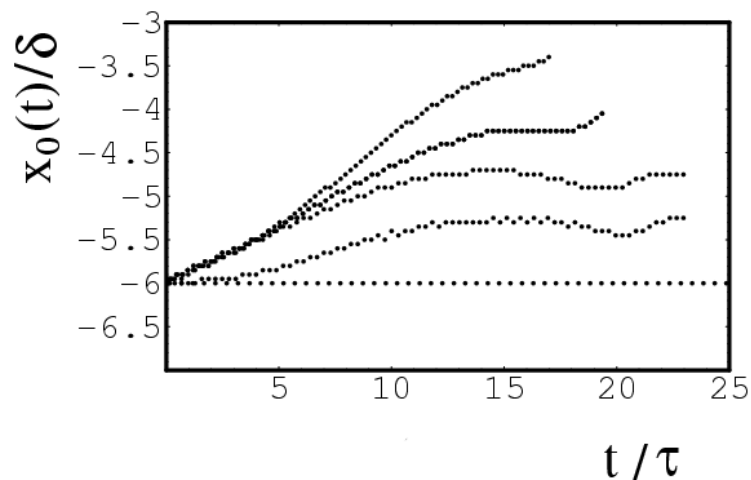


FIG .8: The x-coordinate of the vortex core $x_0(t)$ as a function of time for different values of δ . Starting from the uppermost curve, the value of δ equals 14, 14.25, 15, 18, 20, 45.

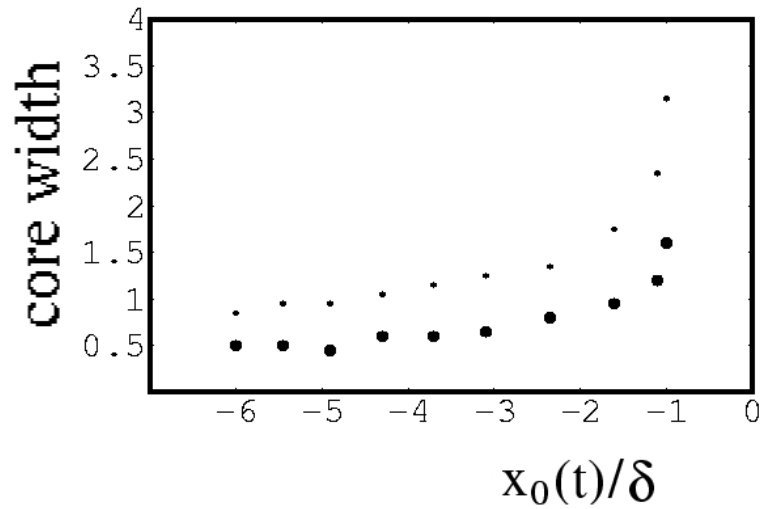


FIG. 9: Thick dots represent the size of the vortex core in units of δ in the x-direction as a function of x_0 , and light dots represent the core size in the y-direction. The width of the core is calculated at the point when the density drops to half of the vortex-free background density.